

See discussions, stats, and author profiles for this publication at: <https://www.researchgate.net/publication/6389738>

Protein Tyrosine Phosphatase Oligomerization Studied by a Combination of ^{15}N NMR Relaxation and ^{129}Xe NMR. Effect of Buffer Containing Arginine and Glutamic Acid

ARTICLE in JOURNAL OF THE AMERICAN CHEMICAL SOCIETY · JUNE 2007

Impact Factor: 12.11 · DOI: 10.1021/ja069144p · Source: PubMed

CITATIONS

14

READS

20

8 AUTHORS, INCLUDING:



David Vidal

Chemotargets SL

15 PUBLICATIONS 324 CITATIONS

SEE PROFILE



Pau Bernado

French Institute of Health and Medical Resea...

79 PUBLICATIONS 2,876 CITATIONS

SEE PROFILE



Oscar Millet

Center for Cooperative Research in Biosciences

61 PUBLICATIONS 1,972 CITATIONS

SEE PROFILE



Miquel Pons

University of Barcelona

170 PUBLICATIONS 3,317 CITATIONS

SEE PROFILE

Protein Tyrosine Phosphatase Oligomerization Studied by a Combination of ^{15}N NMR Relaxation and ^{129}Xe NMR. Effect of Buffer Containing Arginine and Glutamic Acid

Jascha Blobel,[†] Sabine Schmidl,[‡] David Vidal,[†] Lydia Nisius,[‡] Pau Bernadó,[†]
Oscar Millet,^{†,§} Eike Brunner,[‡] and Miquel Pons^{*,†,§}

Contribution from the Laboratory of Biomolecular NMR, Institute for Research in Biomedicine, Parc Científic de Barcelona, Josep Samitier, 1-5, E-08028 Barcelona, Spain, Institut für Biophysik und Physikalische Biochemie, Universität Regensburg, 93040 Regensburg, Germany, and Departament de Química Orgànica, Universitat de Barcelona, Martí i Franquès, 1-11, E-08028 Barcelona, Spain

Received December 29, 2006; E-mail: mpons@ub.edu

Abstract: ^{15}N NMR relaxation and ^{129}Xe NMR chemical shift measurements offer complementary information to study weak protein–protein interactions. They have been applied to study the oligomerization equilibrium of a low-molecular-weight protein tyrosine phosphatase in the presence of 50 mM arginine and 50 mM glutamic acid. These experimental conditions are shown to enhance specific protein–protein interactions while decreasing nonspecific aggregation. In addition, ^{129}Xe NMR chemical shifts become selective reporters of one particular oligomer in the presence of arginine and glutamic acid, indicating that a specific Xe binding site is created in the oligomerization process. It is suggested that the multiple effects of arginine and glutamic acid are related to their effective excluded volume that favors specific protein association and the destabilization of partially unfolded forms that preferentially interact with xenon and are responsible for nonspecific protein aggregation.

Introduction

Weak protein–protein interactions play a key role in the regulation of many biological processes, but their study remains a challenge.¹ These interactions are strongly affected by environmental effects, including the global macromolecular concentration in the cell. They are very sensitive to the experimental conditions, including buffer composition. NMR spectroscopic methods allow the study of transient protein interactions under physiological conditions in atomic detail.² In this article, we report the complementary use of two different NMR techniques, ^{15}N NMR relaxation and ^{129}Xe chemical shift measurements, to study the complex oligomerization equilibria of a low-molecular-weight protein tyrosine phosphatase (lmwPTP).

The interplay of kinases and phosphatases is responsible for the regulation of various signal transduction pathways. Phosphatases can be separated into two families, referred to as transmembrane receptor-like PTPs, often consisting of a dual tandem catalytic domain such as CD45, and cytoplasmic PTPs, of which lmwPTPs are members. lmwPTP takes part, among others, in platelet-derived growth factor (PDGF)-induced mi-

togenesis³ and insulin-mediated mitotic and metabolic signaling.⁴ Phosphatase regulation is much less well known than that of kinases. Relocalization and catalytic inhibition through inter- and intracellular events play a crucial role.⁵ It could be shown for a EGF Receptor-CD45 chimera that the dimerization of its cytosolic domain bearing the catalytic site, stimulated through the addition of EFG, impaired its functional ability to support T cell receptor signaling.⁶ Dimerization of lmwPTP has also been detected and demonstrated by a variety of physicochemical techniques, including ultracentrifugation,⁷ concentration-dependent NMR chemical shift changes,⁸ and NMR relaxation.⁹ The S19A mutant of bovine lmwPTP was crystallized as a dimer with pseudo-2-fold symmetry.⁷ The dimer interface includes the mutual interaction of the enzyme active site of one molecule with tyrosine residues 131 and 132 of a second molecule. Therefore, the active site is blocked in the dimer, and this species is intrinsically inactive. Reversible formation of (inactive) dimers from (active) monomers has been suggested as a possible regulation mechanism for lmwPTP and other enzymes.^{7,10}

(3) Chiarugi, P.; Cirri, P.; Marra, F.; Raugei, G.; Fiaschi, T.; Camici, G. *J. Biol. Chem.* **1998**, *273*, 6776–6785.

(4) Chiarugi, P.; Cirri, P.; Marra, F.; Raugeand, G. *Biochem. Biophys. Res. Commun.* **1997**, *238*, 676–682.

(5) Weiss, A.; Schlessinger, J. *Cell* **1998**, *94*, 277–280.

(6) Desai, D. M.; Sap, J.; Schlessinger, J.; Weiss, A. *Cell* **1993**, *73*, 541–554.

(7) Taberner, L.; Evans, B. N.; Tishmack, P. A.; Van Etten, R. L.; Stauffacher, C. V. *Biochemistry* **1999**, *38*, 11651–11658.

(8) Akerud, T.; Thulin, E.; Van Etten, R. L.; Akke, M. *J. Mol. Biol.* **2002**, *322*, 137–152.

(9) Bernadó, P.; Akerud, T.; De la Torre, J. G.; Akke, M.; Pons, M. *J. Am. Chem. Soc.* **2003**, *125*, 916–923.

(10) Minton, A. P.; Wilf, J. *Biochemistry* **1981**, *20*, 4821–4826.

[†] Institute for Research in Biomedicine.

[‡] Universität Regensburg.

[§] Universitat de Barcelona.

^{*} Present address: Structural Biology Unit, CIC bioGUNE, Bizkaia Technology Park, Building 801A, 48160 Derio, Spain.

(1) Nooren, I. M. A.; Thornton, J. M. *J. Mol. Biol.* **2003**, *325*, 991–1018.

(2) Takeuchi, K.; Wagner, G. *Curr. Opin. Struct. Biol.* **2006**, *16*, 109–117.

Phosphorylation of residues 131 and/or 132 has been reported to increase the enzyme activity *in vivo*.¹¹ The phosphorylated species becomes a substrate of a second lmwPTP molecule, and the auto-dephosphorylation mechanism enables lmwPTP to self-regulate.¹² The structure of the dimer resembles the end product of the dephosphorylation reaction, connecting the two possible regulation mechanisms.

We had previously used ¹⁵N NMR relaxation at different protein concentrations to study the oligomerization equilibria of lmwPTP. X-ray structures of the lmwPTP monomer and dimer were used to predict the relaxation rates of the individual species using hydrodynamic calculations.^{9,13} These studies proved the existence of at least one higher molecular weight species that was compatible with a tetramer (i.e., a dimer of dimers). The formation of larger oligomers involving lmwPTP dimers should increase the cooperativeness of the transition between active and inactive forms in a putative regulation process and would make the system more sensitive to crowding effects *in vivo*. This could reduce the optimal protein concentration for regulation by an oligomerization mechanism to values closer to the physiological concentrations.

¹²⁹Xe NMR chemical shifts have been used to detect the presence of cavities that can act as xenon binding sites^{14–16} or conformational changes, as in the case of maltose binding protein.¹⁷ Xenon atoms encapsulated in cages have been proposed as biosensors to monitor protein interactions.¹⁸ As a silent observer of molecular interaction events, ion and small-molecule binding to target proteins has been studied for the *Escherichia coli* chemotaxis Y protein, where the interaction of the ligands blocks the interaction site for xenon.¹⁹ We reasoned that protein–protein interactions could be also studied using ¹²⁹Xe NMR, since macromolecular interactions may either bury hydrophobic surfaces that are sensed by xenon or generate new xenon binding sites at the interface of the interacting proteins. In order to test this hypothesis, we have measured ¹²⁹Xe NMR chemical shifts in the presence of increasing concentrations of lmwPTP under the same conditions at which NMR relaxation measurements were carried out. By studying the same oligomerization process using two independent NMR techniques, we provide a mutual validation of both methods.

Nonspecific protein aggregation may obscure information about specific interactions, especially at high protein concentrations. In a recent publication, Golovanov et al. reported that the addition of 50 mM arginine and 50 mM glutamic acid to the usual buffers used in NMR studies of proteins resulted in an increase in solubility, a decrease in line broadening associated with nonspecific aggregation, and an increase in the chemical

stability of many proteins.²⁰ The authors suggested that specific protein–protein interactions would not be affected by the presence of arginine and glutamic acid (RE). We have carried out NMR relaxation and ¹²⁹Xe chemical shift studies of the lmwPTP system at different concentrations in the presence and in the absence of RE. In this article, we show that the presence of RE enhances the formation of specific lmwPTP oligomers and reduces nonspecific Xe–protein interactions, making ¹²⁹Xe chemical shifts selective for a single lmwPTP oligomer.

Materials and Methods

Protein Expression. pET-11d vector, harboring the wild-type lmwPTP gene, was transformed into *E. coli* BL21(DE3) cells and expressed in LB or minimum media as described before.²¹ The lysate was pumped onto a cation-exchange column (SP Sepharose High Performance) equilibrated in buffer A (10 mM potassium acetate, 10 mM sodium phosphate, 60 mM NaCl, 1 mM EDTA, pH 4.7) containing 1 mM dithiothreitol (DTT). Elution was achieved by increasing the phosphate concentration to 150 mM, the pH to 5.1, and the DTT concentration to 5 mM. Final purification by size exclusion chromatography (Superdex 75) using buffer A containing 2 mM DTT resulted in pure protein solution, as confirmed by SDS–PAGE and mass spectrometry. All NMR experiments were carried out at 310 K in standard buffer (200 mM potassium phosphate, 10 mM tris(2-carboxyethyl)phosphine hydrochloride (TCEP·HCl), 3 mM sodium azide, pH 6.00), with or without 50 mM RE. Buffer exchange was achieved by three cycles of a 15 fold up-concentration and dilution process using the final buffer, resulting in an exchange of >99.5%. Protein concentrations were determined by UV absorption at 280 nm by diluting the desired solution 1/40 in a buffer containing 6 M guanidinium chloride and 20 mM sodium phosphate at pH 6.5. The average of three measurements of pure buffer was subtracted from the average of three measurements of protein solution, and the concentration was determined according to the equation $1 \text{ AU}(A_{280}) = 0.84 \pm 0.05 \text{ g/L}$.⁸

NMR Relaxation Measurements. From a single expression batch, bovine lmwPTP was prepared in standard buffer with (RE buffer) or without (non-RE buffer) 50 mM RE. NMR relaxation and HSQC experiments were performed on a Bruker 800 MHz spectrometer at 310 K. Longitudinal and transverse ¹⁵N relaxation rates were measured in RE-containing and RE-free buffer at the seven concentrations of 1.11, 0.73, 0.55, 0.48, 0.41, 0.34, and 0.17 mM and the four concentrations of 1.09, 0.60, 0.34, and 0.17 mM, respectively. Spectral widths (complex data points) were 4808 Hz (1024) in ω_2 (¹H) and 3243 Hz (250) in ω_1 (¹⁵N). R_1 rates were determined using the following sequence of relaxation delays (in ms): 10, 1500, 50, 1000, 100, 500, and 220. The recovery delay was 1.5 s. The relaxation delays (in ms) used to determine R_2 rates were 150, 22, 82, 42, 102, 62, and 122. The recovery delay was 2 s. Spectra were processed with NMRPipe.²² Peak picking was performed using the R_1 experiment with the shortest delay (10 ms) recorded for the highest lmwPTP concentration in non-RE buffer. The relaxation rates were calculated from the peak intensities using an in-house-designed program running in Matlab. To exclude unnoticed precipitation during the accumulation of the relaxation experiments, HSQC spectra were recorded before and after each series of measurements. Peak positions and intensities were unchanged.

Analysis of the Oligomerization Equilibria. Relaxation data were modeled assuming fast equilibration between three species: monomer, dimer, and an isotropic tetramer (a dimer of dimers). Within this model, observed R_1 and R_2 relaxation rates for each residue, j , are the

- (11) Tailor, P.; Gilman, J.; Williams, S.; Couture, C.; Mustelin, T. *J. Biol. Chem.* **1997**, *272*, 5371–5374.
- (12) Schwarzer, D.; Zhang, Z.; Zheng, W.; Cole, P. A. *J. Am. Chem. Soc.* **2006**, *128*, 4192–4193.
- (13) Bernado, P.; Garcia de la Torre, J.; Pons, M. *J. Biomol. NMR* **2002**, *23*, 139–150.
- (14) Gröger, C.; Möglich, A.; Pons, M.; Koch, B.; Hengstenberg, W.; Kalbitzer, H. R.; Brunner, E. *J. Am. Chem. Soc.* **2003**, *125*, 8726–8727.
- (15) Dubois, L.; Da Silva, P.; Landon, C.; Huber, J. G.; Ponchet, M.; Vovelle, F.; Berthault, P.; Desvaux, H. *J. Am. Chem. Soc.* **2004**, *126*, 15738–15746.
- (16) Rubin, S. M.; Lee, S.-Y.; Ruiz, E. J.; Pines, A.; Wemmer, D. E. *J. Mol. Biol.* **2002**, *322*, 425–440.
- (17) Rubin, S. M.; Spence, M. M.; Dimitrov, I. E.; Ruiz, E. J.; Pines, A.; Wemmer, D. E. *J. Am. Chem. Soc.* **2001**, *123*, 8616–8617.
- (18) Lowery, T. J.; García, S.; Chavez, L.; Ruiz, E. J.; Wu, T.; Brotin, T.; Dutasta, J.-P.; King, D. S.; Schultz, P. G.; Pines, A.; Wemmer, D. E. *ChemBioChem* **2006**, *7*, 65–73.
- (19) Lowery, T. J.; Doucleff, M.; Ruiz, E. J.; Rubin, M. S.; Pines, A.; Wemmer, D. E. *Protein Sci.* **2005**, *14*, 848–855.

- (20) Golovanov, A. P.; Hautbergue, G. M.; Wilson, S. A.; Lian, L.-Y. *J. Am. Chem. Soc.* **2004**, *126*, 8933–8939.
- (21) Wo, Y.-Y. P.; Zhou, M.-M.; Stevis, P.; Davis, J. P.; Zhang, Z.-Y.; Van Etten, R. L. *Biochemistry* **1992**, *31*, 1712–1721.
- (22) Delaglio, F.; Grzesiek, S.; Vuister, G. W.; Zhu, G.; Pfeifer, J.; Bax, A. *J. Biomol. NMR* **1995**, *6*, 277–293.

population-weighted averages of R_1 and R_2 of this residue in the different species, i :²³

$$R_{x,j} = \sum_i f_i R_{x,j}^i \quad (1)$$

with $x = 1, 2$ and f_i representing the molar fraction of the protein in the different species i . For the monomer and the dimer, the values for $R_{x,j}^M$ and $R_{x,j}^D$ were calculated from the corresponding 3D structures using HydroNMR,²⁴ whereas R_1 and R_2 for all residues in the tetramer were assumed to be the same and were treated as two adjustable parameters. Additional adjustable parameters in this model are the dissociation constants of the dimer and the tetramer that determine the f_i values at different protein concentrations. Minimization of χ^2 provides an estimate of the dissociation constants from the concentration-dependent relaxation data:

$$\chi^2 = \sum_c \sum_j \frac{[(R_2/R_1)_{c,j}^{\text{exp}} - (R_2/R_1)_{c,j}^{\text{calc}}]^2}{[\sigma(R_2/R_1)_{c,j}^{\text{exp}}]^2} \quad (2)$$

where the summation runs over all protein concentrations, c , and a filtered list of residues j (see below). $\sigma(R_2/R_1)$ is the experimental error of the measured R_2/R_1 .

To minimize the effect of local motion, experimental and calculated R_2/R_1 ratios were compared instead of the individual relaxation rates.²⁵

Minimization was carried out using an in-house-developed genetic algorithm. Convergence was confirmed by repeating the procedure 50 times from random starting populations of 10 000 individuals. The error in the parameters was calculated by a Monte Carlo analysis using 100 artificial data sets obtained from the back-calculated $(R_2/R_1)_{c,j}^{\text{calc}}$ values to which a Gaussian random noise with amplitude $\sigma(R_2/R_1)_{c,j}^{\text{exp}}$ was added.

Data Filtration. The first three residues, which are not present in the structure of the dimer (1COE), were not used. Furthermore, residues 5, 84, 105, 107, 108, 109, 110, and 157, reported to have hetNOEs ≤ 0.6 , were excluded.⁸ Points with experimental errors in R_2/R_1 larger than 25% were also excluded from the calculations.

Extraction of global correlation times from relaxation data is based on the assumption of a rigid structure perfectly described by the model derived from X-ray and the absence of contributions from relaxation mechanisms other than dipole–dipole and chemical shift anisotropy with a known and constant CSA tensor. Those assumptions may break down for some particular NH groups, but they are expected to be fulfilled by the majority. In order to identify the relevant set of residues, a preliminary minimization was carried out after the initial filtration. Residues showing deviations in R_2/R_1 larger than 25% of the experimental values were removed from the final minimization. The final dataset contained 607 R_2/R_1 values measured in RE buffer covering seven lmwPTP concentrations and 331 values measured in the absence of RE covering four protein concentrations.

Hydrodynamic Calculations. Predicted values of R_2/R_1 for monomer and dimer lmwPTP were calculated by HydroNMR²⁴ using the PDB structures 1PNT²⁶ and 1COE,⁷ respectively, with an atomic element radius of 3.3 Å.¹³

Rotational diffusion is sensitive to the viscosity of the solvent. The viscosity of six buffers with different equimolar concentrations of arginine and glutamic acid between 0 and 50 mM was determined experimentally using a capillary viscosimeter calibrated with pure water at 310 K. The viscosity increases linearly with the concentration of

arginine and glutamic acid (data not shown). The experimentally determined viscosities of non-RE and 50 mM RE buffer are 0.7189 and 0.7488 cP, respectively, at 310 K. For hydrodynamic calculations, the calibration of the value of the atomic element radius had previously been carried out employing data obtained in a variety of standard buffers using the viscosity of water ($\eta = 0.6915$ cP at 310 K).¹³ Consistently, we have taken the viscosity of pure water for calculating rotational diffusion in non-RE buffer. For the buffer containing RE, we used $\eta = 0.7203$ cP, which results from multiplying the viscosity of pure water by the ratio of the experimentally determined viscosities of 50 mM RE and non-RE buffers.

¹²⁹Xe Chemical Shift Measurements. ¹²⁹Xe chemical shifts were measured in the same protein concentration range as the NMR relaxation experiments. At the highest concentration of 1.11 mM lmwPTP in RE buffer, sample precipitation was observed after some days, preventing the measurement of ¹²⁹Xe chemical shifts. For the other concentrations, no precipitation occurred. The highest protein concentration was measured by UV/vis spectroscopy as described above. The lower concentrations were prepared by dilution of the concentrated sample with buffer. Xenon loading was performed by directly pressurizing the samples in an apparatus similar to the one described earlier,²⁷ always using the same xenon pressure of 0.5 MPa. According to the reported molar fraction solubility of 7.92×10^{-5} for xenon at 101.3 kPa in pure water, the concentration of dissolved xenon is approximately 22 mM. Note that the real concentration in the samples under study may be slightly different due to the presence of lmwPTP and the buffer constituents. It is important to mention that our apparatus allows for direct pressurization of the samples with xenon at room temperature without the need for any freeze–thaw procedure. This prevents nonspecific aggregation, which may otherwise occur for this protein. The loading was checked volumetrically after each measurement. Within an error well below 5%, identical amounts of xenon were leaving the samples. This test procedure proved the correctness of xenon loading as well as the tightness of the apparatus. The chemical shift of dissolved ¹²⁹Xe was referenced relative to the chemical shift of xenon gas at zero pressure. The induced chemical shift, $\Delta\delta$, was measured relative to the protein-free original buffer used for the protein solutions under study. This allows for the determination of the induced chemical shift $\Delta\delta$ with the required precision. The line width of the ¹²⁹Xe NMR signals increases in the presence of protein, as previously described.^{15,16} However, for our system it remains well below 15 Hz, even for the higher protein concentrations, allowing very accurate $\Delta\delta$ measurements with an experimental error of ± 0.02 ppm. ¹²⁹Xe chemical shift measurements were performed at 139.05 MHz (11.7 T corresponding to 500 MHz ¹H NMR frequency) and 310 K. The temperature was calibrated and controlled to within ± 0.1 K. The ¹H/¹⁵N xenon-induced chemical shift mapping experiments are based on standard ¹H–¹⁵N HSQC spectroscopy and were also carried out at 11.7 T field strength. A xenon pressure of 1.2 MPa was applied to the samples for these experiments.

Results

¹⁵N NMR Relaxation of lmwPTP in RE Buffer. Longitudinal and transverse relaxation rates were measured at pH 6.00 and 310 K for seven lmwPTP concentrations in the presence of 50 mM arginine and 50 mM glutamic acid. Experimental values for the relaxation rates of individual amide ¹⁵N nuclei at different concentrations are given as Supporting Information. Figure 1 shows the average values of R_2/R_1 for residues that passed the selection criteria ($\langle R_2/R_1 \rangle$) as a function of lmwPTP concentration.

As previously observed for this protein in RE-free buffer, $\langle R_2/R_1 \rangle$ increases with the protein concentration.⁸ This indicates

- (23) Fushman, D.; Cahill, S.; Cowburn, D. *J. Mol. Biol.* **1997**, 266, 173–194.
 (24) García de la Torre, J.; Huertas, M. L.; Carrasco, B. *J. Magn. Reson.* **2000**, 147, 138–146.
 (25) Tjandra, N.; Feller, S. E.; Pator, R. W.; Bax, A. *J. Am. Chem. Soc.* **1995**, 117, 12562–12566.
 (26) Zhang, M.; Van Etten, R. L.; Stauffacher, C. V. *Biochemistry* **1994**, 33, 11097–11105.

- (27) Baumer, D.; Fink, A.; Brunner, E. *Z. Phys. Chem.* **2003**, 217, 289–293.

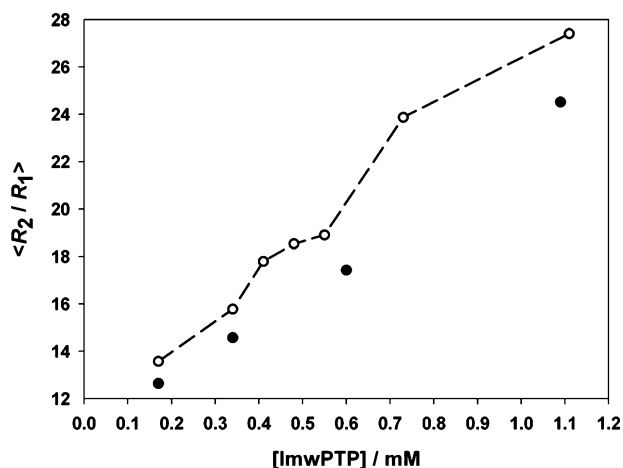


Figure 1. Average ^{15}N R_2/R_1 ratios of lmwPTP determined as a function of protein concentration measured in the presence of 50 mM arginine and 50 mM glutamic acid at pH 6.00 and 310 K (open circles connected by dashed line). Data at four concentrations of the same batch of protein measured in RE-free buffer are included for comparison (filled circles). The data measured in 50 mM RE-containing buffer have been corrected for changes in viscosity as described in the Materials and Methods section.

the presence of species with longer correlation times at increasing lmwPTP concentrations. The curve shows a monotonic increase that can be roughly described as two consecutive sigmoidal curves. For comparison, relaxation was measured at four concentrations of the same protein batch in the absence of RE. Since the viscosity of RE-containing buffers is higher, the RE data shown in Figure 1 were scaled to the viscosity of RE-free buffer. Even after correction for changes in viscosity, the values measured in the presence of RE are higher than those in RE-free buffer. This observation suggests an increased contribution from larger species in RE buffer. The effect is more pronounced at higher protein concentrations, suggesting a displacement of the lmwPTP oligomerization equilibrium.

Accounting for macroscopic viscosity is a first-order correction that does not take into account possible effects such as weak interactions of RE with the protein or small changes in the compactness of the protein induced by RE. These terms would contribute to what is known as microviscosity. However, a convincing agreement could be observed between the experimental correlation times obtained from relaxation rates measured in 45 mM RE and the values predicted from the three-dimensional structure of a protein which is not involved in oligomerization equilibria.²⁸ This observation confirms that microviscosity is not responsible for the changes observed for lmwPTP.

The concentration of the different oligomers can be derived from the experimental relaxation rates of individual NH sites and the site-specific relaxation rates of the individual species. Those can be accurately predicted from the X-ray structures of monomeric and dimeric lmwPTP using HydroNMR²⁴ under the assumption of rigid body motion. Assuming fast equilibrium, the experimental relaxation rates are weighted averages of the contributions of the different species. The ensemble of relaxation rates measured at different protein concentrations can be used to fit a model describing the oligomerization equilibria. This procedure was previously used to demonstrate the formation

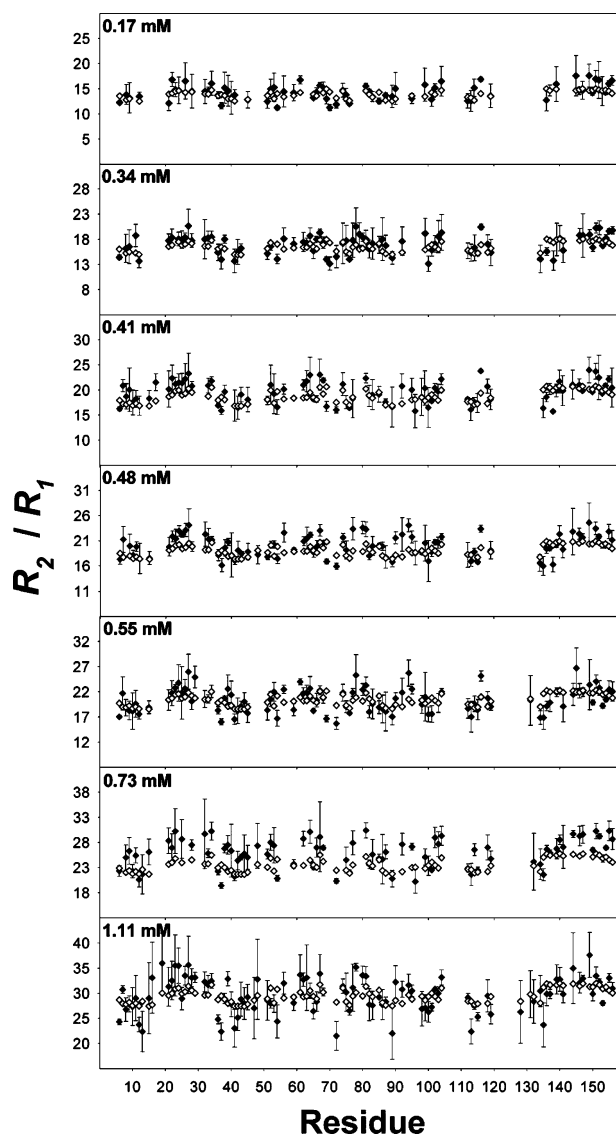


Figure 2. Experimental and calculated ^{15}N R_2/R_1 values in 50 mM RE-containing buffer at different protein concentrations. Experimental data are shown as filled diamonds with their corresponding error. Calculated values, shown as open symbols, correspond to the best fit to the monomer–dimer–tetramer model. Only the 607 experimental data points that passed the filtering criteria are shown.

of at least one additional oligomer of lmwPTP, being consistent with a tetramer.⁹

The monomer–dimer–tetramer model has four adjustable parameters: the global relaxation rates R_1 and R_2 of the tetramer, referred to as R_{1T} and R_{2T} , and the dissociation constants of the dimer (K_D) and of the tetramer (K_T). The dissociation constant for the tetramer is defined as

$$K_T = [\text{D}]^2/[\text{T}] \quad (3)$$

The values of the parameters that give the best fit to the experimental data are $K_D = 4.18 \pm 0.07$ mM, $K_T = 0.074 \pm 0.006$ mM, $R_{1T} = 0.44 \pm 0.03$ s⁻¹, and $R_{2T} = 38.33 \pm 0.74$ s⁻¹, with a reduced χ^2 value of 5.036. Experimental and back-calculated R_2/R_1 values in RE-containing buffer are compared in Figure 2. Clearly, a good agreement is observed for concentrations up to 0.55 mM. Systematic deviations above 0.73 mM suggest that additional aggregation, not accounted for by

(28) Fedoroff, O. Y.; Townson, S. A.; Golovanov, A. P.; Baron, M.; Avis, J. *M. J. Biol. Chem.* **2004**, 279, 34991–35000.

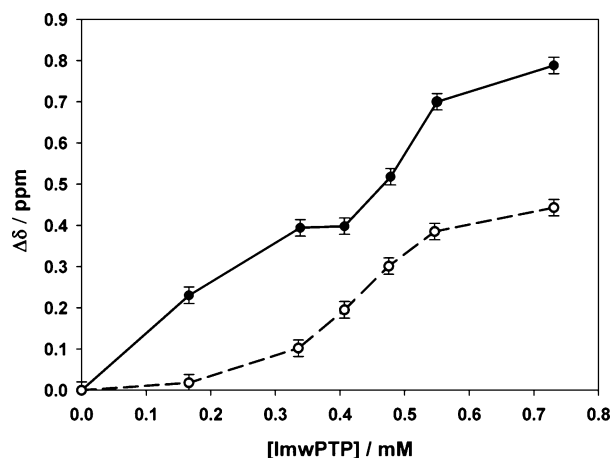


Figure 3. ^{129}Xe chemical shifts in the presence of lmwPTP with respect to protein-free buffer. Filled circles show data recorded in RE-free buffer, and open circles show data recorded in RE-containing buffer.

the monomer–dimer–tetramer model, occurs at high concentrations in the presence of 50 mM RE.

If the measurements at the two highest protein concentrations are not considered, the same value for K_D (4.19 mM) and a slightly larger value for K_T (0.186 mM) are obtained, confirming the presence of the three species even at low lmwPTP concentrations. The reduced χ^2 value decreases to 4.705.

Protein-Induced ^{129}Xe NMR Chemical Shifts. The lmwPTP-induced ^{129}Xe NMR chemical shift, $\Delta\delta$, measured as the difference in Xe NMR signal between protein-containing sample and protein-free buffer, is plotted as a function of lmwPTP concentration in Figure 3. The two curves correspond to the effect of protein in the presence and in the absence of 50 mM RE.

^{129}Xe NMR chemical shifts typically show a strictly linear dependence on the concentration of the added protein.^{16,17,29–31} However, in the case of lmwPTP, ^{129}Xe chemical shifts clearly show a nonlinear dependence on the total protein concentration. In addition, the curves measured in the presence and in the absence of RE are very different. The total ^{129}Xe chemical shift change caused by any given protein concentration is higher in RE-free than in RE-containing buffer. The overall smaller effect observed in the presence of RE emphasizes the sigmoidal shape of the curve, with a pronounced chemical shift increase from 0.3 to 0.6 mM lmwPTP. Interestingly, a clear increase in $\langle R_2/R_1 \rangle$ is observed at the same protein concentrations (see Figure 1). In the case of RE-free buffer, a comparable increase in chemical shift is detected at higher protein concentrations.

^{129}Xe NMR Chemical Shift Response to Different lmwPTP Oligomers in RE Buffer. The very unusual nonlinear response of ^{129}Xe chemical shifts toward the addition of lmwPTP in the presence of RE can be related to the oligomerization equilibria calculated from ^{15}N NMR relaxation. Hereby, it is assumed that each species interacts differently with ^{129}Xe .

Assuming a linear response of the ^{129}Xe chemical shift with respect to the concentration of the individual species present,

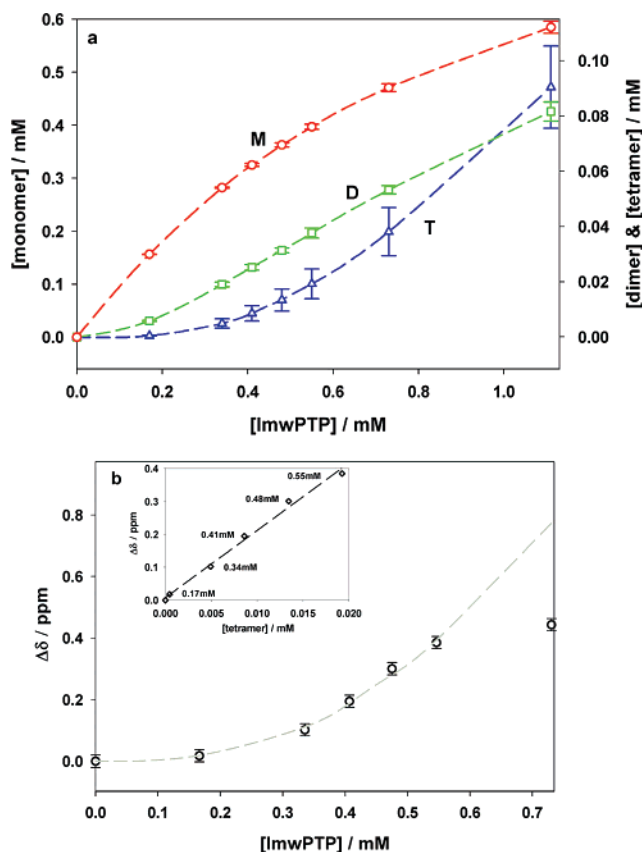


Figure 4. (a) Concentration of the individual lmwPTP species calculated from ^{15}N NMR relaxation in RE-containing buffer as a function of total protein concentration. Note the different scales used for monomer (red circles, left scale), dimer (green squares, right scale), and tetramer (blue triangles, right scale). (b) Comparison of experimental protein-induced ^{129}Xe chemical shifts with the best fit to the relaxation-derived monomer–dimer–tetramer model. The inset shows the linear dependence of $\Delta\delta$ on the concentration of tetramer, calculated from the total protein concentration and the relaxation-derived dissociation constants.

the lmwPTP-induced ^{129}Xe chemical shift, $\Delta\delta$, at a certain protein concentration, i , is given by

$$\Delta\delta = \sum \alpha_i c_i \quad (4)$$

where c_i is the concentration of the individual species i .³⁰ Values of c_i can be obtained from the equilibrium constants providing the best fit to the relaxation data. The values of α_i are derived from fitting the experimental chemical shift values as a function of the total protein concentration.

In Figure 4a, the concentration of the individual species, derived from the relaxation rate analysis using all the concentrations measured, is shown as a function of the total lmwPTP concentration.

Figure 4b shows a very good agreement between observed and computed ^{129}Xe chemical shifts for lmwPTP concentrations up to 0.6 mM when using $\alpha_M = 0.026 \pm 0.012 \text{ ppm} \cdot \text{mM}^{-1}$, $\alpha_D = 0.90 \pm 1.20 \text{ ppm} \cdot \text{mM}^{-1}$, and $\alpha_T = 17.2 \pm 3.1 \text{ ppm} \cdot \text{mM}^{-1}$. The lmwPTP concentration of 0.6 mM corresponds to the upper limit of the range of validity of the monomer–dimer–tetramer model for the interpretation of relaxation data. According to this analysis, ^{129}Xe is almost exclusively detecting the presence of lmwPTP tetramers in RE-containing buffer. The large uncertainty in α_D reflects the combination of a weak

(29) Rubin, S. M.; Spence, M. M.; Pines, A.; Wemmer, D. E. *J. Magn. Reson.* **2001**, *152*, 79–86.

(30) Rubin, S. M.; Spence, M. M.; Goodson, B. M.; Wemmer, D. E.; Pines, A. *Proc. Natl. Acad. Sci. U.S.A.* **2000**, *97*, 9472–9475.

(31) Locci, E.; Dehouck, Y.; Casu, M.; Saba, G.; Lai, A.; Luhmer, M.; Reisse, J.; Bartik, K. *J. Magn. Reson.* **2001**, *150*, 167–174.

interaction with Xe and a low concentration of the dimer at equilibrium.

The slope α of the protein-induced ^{129}Xe NMR chemical shifts depends on the specific protein and its folding state. The α value for proteins with only nonspecific xenon–protein interactions was found to increase linearly with the size of the protein, i.e., the number of amino acids, N . In order to classify the type of xenon–protein interactions, it is therefore reasonable to introduce the ratio α/N . Typically, nonspecific interactions give rise to α/N values well below 0.005 ppm per millimole of residue.^{29,30} Larger protein-induced shifts reflect specific interactions.

The values of α/N for the monomer, dimer, and tetramer are $\alpha_M/N = (1.6 \pm 0.7) \times 10^{-4}$, $\alpha_D/N = (2.8 \pm 3.7) \times 10^{-3}$, and $\alpha_T/N = (2.7 \pm 0.4) \times 10^{-2}$ ppm per millimole of residue. By using the concentrations derived from the analysis of relaxation data obtained from the five lowest concentrations, the calculated α_D/N and α_T/N values increase to 8×10^{-3} and 4×10^{-2} ppm per millimole of residue, while the effect of the monomer becomes negligible.

The value of 0.03–0.04 ppm per millimole of residue for the tetramer is well above the limit considered to be indicative of specific interactions, suggesting the presence of a specific xenon binding site in this oligomer that is not present in the monomeric protein. Indeed, no cavities that could accommodate Xe, or even a smaller probe atom like argon, could be observed in the crystal structure of lmwPTP. For the lmwPTP dimer, α_D/N has a large uncertainty, but even its upper limit would just be close to the borderline value of ca. 0.005 ppm per millimole of residue, much lower than the one obtained for the tetramer. The appearance of a new Xe binding site, not present in the monomer or in the dimer, strongly suggests that the new site is formed at the interface between the two dimers forming the tetrameric species.

Xenon binding into hydrophobic pockets pre-existing on the surface of the protein usually results in the observation of induced chemical shifts for ^1H , ^{15}N , or ^{13}C nuclei of the protein close to the hydrophobic cavity.^{14–16} However, no significant chemical shift changes were observed in ^1H – ^{15}N HSQC spectra obtained at high Xe pressure for protein concentrations up to 1 mM (data not shown). The absence of a specific binding site in the major species present at low concentrations (monomer and dimer) is consistent with this observation. At higher concentrations, the tetramer is still a minor species, and any effect would be scaled by its molar fraction. This is a major difference between chemical shift perturbation measurements based on protein observation, and ^{129}Xe chemical shift measurements. The former are simply weighted by the concentration of the different species, while the latter are amplified by the sensitive response of ^{129}Xe to specific binding.

Specific versus Nonspecific Protein-Induced ^{129}Xe NMR Shifts: Effect of RE. The protein-induced ^{129}Xe chemical shift versus protein concentration profile is very different in the presence and in the absence of 50 mM RE. At low protein concentrations, where oligomer formation is negligible, ^{129}Xe chemical shifts are dominated by the nonspecific interaction of xenon with the lmwPTP monomer. The initial slope of the $\Delta\delta$ vs [lmwPTP] curve in RE-free buffer is ca. 1.15 ppm·mM^{−1}, corresponding to a relatively high value of 0.007 ppm per millimole of residue, still close to, although larger than, the

expected value for nonspecific interactions (0.005 ppm per millimole of residue). These interactions are largely suppressed by the addition of RE, as shown by the much lower initial slope of the curve in RE buffer. This suggests that one of the effects of RE is to shield or bury exposed regions on the protein surface, to which Xe may weakly bind. On the other hand, specific binding to cavities created in the oligomerization interface is not affected by the addition of RE; therefore, ^{129}Xe chemical shifts become a selective reporter of one of the high-molecular-weight species.

Oligomer-specific interactions may also explain the deviations from linearity in the $\Delta\delta$ versus [lmwPTP] for RE-free buffer. Indeed, experimental deviations of individual points from the regression line show a sigmoidal shape, resembling the one observed in the presence of RE, although displaced to higher concentrations. Thus, tetramers are formed in both cases, although they start to appear at lower protein concentrations in RE-containing buffer.

Effect of RE on the lmwPTP Oligomerization Equilibria.

A comparison of lmwPTP relaxation data in the presence and in the absence of RE also suggests that RE shifts the oligomerization equilibria of lmwPTP, favoring the formation of higher order oligomers. A quantitative assessment of this effect can be obtained by comparing the dissociation constants of lmwPTP dimer and tetramer extracted from concentration-dependent relaxation data in the presence and in the absence of RE. RE-free data consisted of 331 data points obtained at four different protein concentrations. Although the number of lmwPTP concentrations measured in RE-free buffer is less than in the case of RE-containing buffer, the calculated values of the R_2/R_1 ratio for the isotropic (tetramer) species are fully consistent with each other as well as the previously calculated correlation time of 25.5 ns.⁹ The fitted (expected) ratios are 86.7 ± 6.8 (90.7) in the presence of RE and 74.6 ± 22.6 (83.6) in RE-free buffer. The ratio between the R_2/R_1 values with and without RE (1.16) is in good agreement with the square of the ratio of the viscosities of the two buffers (1.08).

K_D and K_T values of $6.10 \pm 0.58 \text{ mM}^{-1}$ and $0.071 \pm 0.028 \text{ mM}^{-1}$, with $R_{1T} = 0.46 \pm 0.10 \text{ s}^{-1}$ and $R_{2T} = 34.33 \pm 3.11 \text{ s}^{-1}$, were obtained by fitting to the monomer–dimer–tetramer model. The K_D and K_T values can be compared with those obtained in the presence of RE ($K_D = 4.18 \pm 0.07 \text{ mM}$, $K_T = 0.074 \pm 0.006 \text{ mM}$). According to these values, the dimer is more stable in the presence of RE, although the difference in K_T values is not significant. However, as the concentrations of tetramer and dimer are related, the overall effect of the addition of RE results in an increase in the concentrations of both the dimer and the tetramer.

The molar fractions of lmwPTP in the different oligomers in the presence and in the absence of RE are presented in Figure 5.

Discussion

We have shown that the oligomerization of lmwPTP can be described as a concentration-dependent dynamic equilibrium between monomers and specific oligomers, especially dimers and tetramers. The analysis of the variation of R_2/R_1 with the protein concentration allows the concentrations of the different oligomers to be determined. Interestingly, a completely different NMR spectroscopic parameter, namely the protein-induced ^{129}Xe

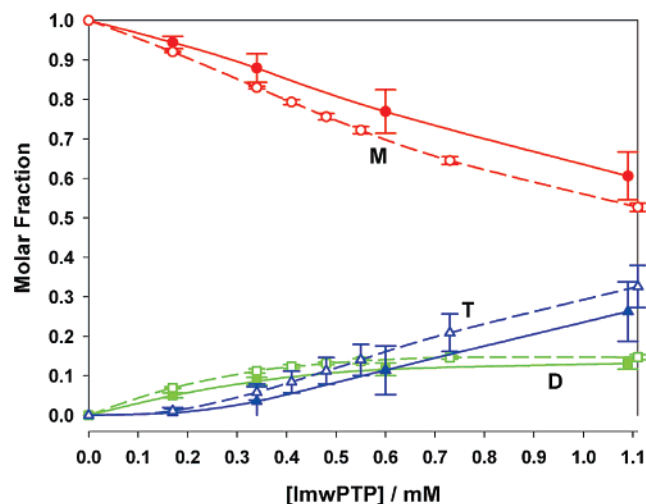


Figure 5. Molar fraction of lmwPTP present in the different oligomeric species at equilibrium in RE-containing buffer (open symbols and dashed lines) and in RE-free buffer (filled symbols and continuous lines): monomer, red circles; dimer, green squares; tetramer, blue triangles.

NMR chemical shift, $\Delta\delta$, also turns out to be a sensitive reporter of lmwPTP oligomerization.

The exquisite sensitivity of ^{129}Xe chemical shifts makes this nucleus an excellent reporter of its environment. However, nonspecific weak binding to a variety of substrates complicates the interpretation of the results. We have found that the addition of arginine and glutamic acid (RE) to the buffer, reported to decrease nonspecific aggregation, also modulates the ^{129}Xe chemical shift response as a function of protein concentration. ^{129}Xe chemical shifts show a complex nonlinear response, reflecting the changing composition of the protein solution as a result of concentration-dependent oligomer formation. The interaction of Xe with the different oligomers changes in the presence of RE. While in the absence of RE ^{129}Xe chemical shifts are affected by all the protein species present, the addition of RE causes ^{129}Xe chemical shifts to become selective for one of the lmwPTP oligomers.

Xenon is considered to bind nonspecifically to hydrophobic patches or to disordered regions on protein surfaces. Xe binding to denatured proteins has already been studied.^{29,30} Disordered regions have also been reported to enhance nonspecific protein aggregation.³² The increased protein solubility and reduced nonspecific Xe interactions caused by RE may have a common origin.

One possibility, suggested by Golovanov et al., is a “shielding” of exposed hydrophobic surfaces of proteins by the binding of arginine and glutamic acid.²⁰ However, no chemical shift changes were observed in ^1H – ^{15}N HSQC spectra of lmwPTP in the presence and in the absence of RE.

A second possibility is that both nonspecific Xe binding and protein aggregation involve disordered portions on the protein surface. RE-induced ordering of the protein surface would provide a common explanation for the effect of RE on ^{129}Xe NMR and protein solubility.

The addition of arginine and glutamic acid to the buffer generally increases protein solubility and decreases aggregation, which cause NMR line broadening. As indicated in the original

paper by Golovanov et al., this buffer does not prevent specific protein–protein or protein–DNA interactions.²⁰ In the case of lmwPTP, oligomer formation is not hindered by arginine and glutamic acid mixtures. On the contrary, the equilibrium is shifted toward the oligomeric species, as seen by the analysis of the concentration dependence of ^{15}N relaxation data and ^{129}Xe chemical shifts measured in the presence and in the absence of RE. The origin of this effect is presently under investigation.

Excluded volume effects (molecular crowding) are known to enhance macromolecular association.^{33–35} Another well-described excluded volume effect is enhanced folding, as the unfolded state is more expanded.³⁶ It is well known that partial unfolding is often responsible for nonspecific aggregation and solubility problems. The reported increase in solubility may be accounted for, at least in some cases, by a destabilization of the partially unfolded forms that cause aggregation. This hypothesis would also explain the reported RE-induced resistance toward contaminating proteases, leading to increased long-term protein stability.²⁰ It is known that disordered protein extremes and loops are more susceptible to attack by proteases than the well-folded protein cores. The observed effects of RE on lmwPTP would be consistent with an excluded volume effect, although it is surprising that these effects are observed at concentrations of two low-molecular-weight additives as low as 50 mM.

Excluded volume effects are typically associated with large concentrations of macromolecules, conditions normally found in the cell cytoplasm.³⁷ Excluded volume can also explain the effects of small molecules on protein folding and stability, although large concentrations of cosolute are usually required.^{38–40}

Electrostatic interactions between oppositely charged ions introduce correlations between their positions which have characteristic length scales.^{41,42} For large inter-ionic distances, the presence of the ions can be accounted for by a change in the effective dielectric constant of an effectively homogeneous background. For short distances between ions, the molecular structure of the ionic background becomes apparent.⁴³

The volume occupied by the protein can be considered a perturbation of the minimum energy structure of the structured solvent, and the tendency to reduce this perturbation will appear as an excluded volume effect and favor the formation of oligomers.

Predictions using the dressed interaction site theory for molecular electrolytes, supported by Monte Carlo computer simulations, show that the electrolyte concentration at which the behavior of the correlation function changes from being continuous to oscillating is lowered by several orders of magnitude for nonspherical multisite electrolytes.⁴³ This is expected for the mixture of arginine and glutamic acid and could

(33) Zimmerman, S. B.; Minton, A. P. *Rev. Biophys. Biomol. Struct.* **1993**, *22*, 27–65.

(34) Ellis, R. J. *Curr. Opin. Struct. Biol.* **2001**, *11*, 114–119.

(35) Zhou, H.-X. *J. Mol. Recognit.* **2004**, *17*, 368–375.

(36) Dedmon, M. M.; Patel, C. N.; Young, G. B.; Pielak, G. J. *Proc. Natl. Acad. Sci. U.S.A.* **2002**, *99*, 12681–12684.

(37) Zimmerman, S. B.; Trach, S. O. *J. Mol. Biol.* **1991**, *222*, 599–620.

(38) Shellmann, J. A. *Biophys. J.* **2003**, *85*, 108–125.

(39) Saunders, A. J.; Davis-Searles, P. R.; Allen, D. L.; Pielak, G. J.; Erie, D. A. *Biopolymers* **2000**, *53*, 293–307.

(40) Tadeo, X.; Pons, M.; Millet, O. *Biochemistry* **2007**, *46*, 917–923.

(41) Kjellander, R.; Mitchell, D. J. *J. Chem. Phys.* **1994**, *101*, 603–626.

(42) Bagatella-Flores, A. N.; González-Mozuelos, P. *J. Chem. Phys.* **2002**, *117*, 6133–6141.

(43) González-Mozuelos, P.; Yeom, M. S.; Olvera de la Cruz, M. *Eur. Phys. J.* **2005**, *16*, 167–178.

(32) Otzen, D. E.; Miron, S.; Akke, M.; Oliveberg, M. *Biochemistry* **2004**, *43*, 12964–12978.

therefore explain the observation of typical excluded volume effects, even at low concentrations.

Comparison of the concentration dependence of the lmwPTP-induced ^{129}Xe chemical shift, $\Delta\delta$, and ^{15}N relaxation rates strongly suggests that xenon preferentially binds to lmwPTP tetramers, formed beyond ca. 0.3 mM lmwPTP concentration. The α/N ratio of 0.03 ppm per millimole of residue indicates the presence of specific binding.

Specific binding to a pre-existing cavity does not take place in individual lmwPTP molecules, as evidenced by the absence of chemical shift effects in the ^1H – ^{15}N HSQC spectra of the protein under xenon pressure. Selective binding of xenon to the tetramer requires that the binding site is created in the oligomerization process. The most likely explanation is that the binding site is formed at the interface between different molecules of the tetramer. This may be a property common to many protein oligomers and would make ^{129}Xe chemical shifts a very sensitive probe for protein aggregation. A corresponding observation was already made for another protein, Hha, which forms small amounts of oligomers, detectable as an increase in fluorescence anisotropy (results not shown).⁴⁴

Concluding Remarks

The use of buffers containing arginine and glutamic acid, in addition to increasing protein solubility and decreasing non-specific protein aggregation, is shown to increase the selectivity of ^{129}Xe chemical shifts from nonspecific toward specific xenon–protein interactions. Xenon NMR becomes a useful tool to study protein–protein interactions that generate a hydrophobic

cavity at their interface capable of accommodating a xenon atom. Furthermore, it could be shown that the addition of arginine and glutamic acid shifts the lmwPTP auto-association equilibrium toward the formation of oligomers. It is suggested that this is due to an excluded volume effect arising from the ion-pair nature of the amino acid mixture. The use of this NMR-friendly amino acid mixture may greatly facilitate further studies of crowding effects by NMR.⁴⁵

Acknowledgment. We thank Prof. Van Etten (Purdue University) and Dr. Akke (University of Lund) for providing the lmwPTP clone. This work was supported by funds from the Spanish Ministerio de Educación y Ciencia–FEDER (BIO2004-5436 and GEN2003-20642-C09-04) to M.P. and the ESF (COST D31, WG 0016-05). E.B. gratefully acknowledges financial support from the Deutsche Forschungsgemeinschaft. Thanks are further due to Mr. Liebold (University of Regensburg) for experimental assistance. J.B. is a recipient of a predoctoral fellowship from the Spanish Ministerio de Educación y Ciencia and thanks Prof. Westerhausen (University of Leipzig) for his continuous encouragement and support. NMR time was provided by Scientific and Technical Services, University of Barcelona.

Supporting Information Available: Relaxation rates measured at different concentrations and buffer conditions (plain text). This material is available free of charge via the Internet at <http://pubs.acs.org>.

JA069144P

(44) García, J.; Cordeiro, T.; Nieto, J. M.; Pons, I.; Juárez, A.; Pons, M. *Biochem. J.* **2005**, *388*, 755–762.

(45) Bernadó, P.; García de la Torre, J.; Pons, M. *J. Mol. Recognit.* **2004**, *17*, 397–407.